

1 Fluid pressure above hydrostatic is a hydrologic characteristic of the Salado (and the Castile) that
2 plays a potentially important role in the repository behavior. It is difficult to accurately measure
3 natural pressures in these formations *accurately* because the boreholes or repository excavations
4 required to access the rocks decrease the stress in the region measured. Stress released
5 instantaneously decreases fluid pressure in the pores of the rock, so measured pressures must be
6 considered as a lower bound of the natural pressures. Stress effects related to test location and
7 the difficulty of making long-duration tests in lower-permeability rocks result in higher pore
8 pressures observed to date in anhydrites. The highest observed pore pressures in halite-rich
9 units, near Room Q, *are* is on the order of 9 MPa, whereas the highest pore pressures observed
10 in anhydrite are *approximately* 12.5 MPa (Beauheim et al. 1993, 139; *Beauheim and Roberts*
11 *2002, p. 82*). Far-field pore pressures in halite-rich and anhydrite beds in the Salado at the
12 repository level are expected to be similar because the anhydrites are too thin and of too low
13 permeabilities to have liquid pressures much different than those of the surrounding salt. For
14 comparison, the hydrostatic pressure for a column of brine at the depth of the repository is about
15 7 MPa, and the lithostatic pressure calculated from density measurements in ERDA-9 is about
16 15 MPa.

17 Fluid pressures in sedimentary basins that are much higher or much lower than hydrostatic are
18 referred to as abnormal pressures by the petroleum industry, where they have received
19 considerable attention. In the case of the Delaware Basin evaporites, the high pressures are
20 almost certainly maintained because of the large compressibility and plastic nature of the halite
21 and, to a lesser extent, the anhydrite. The lithostatic pressure at a particular horizon must be
22 supported by a combination of the stress felt by both the rock matrix and the pore fluid. In
23 highly deformable rocks, the portion of the stress that must be borne by the fluid exceeds
24 hydrostatic pressure but cannot exceed lithostatic pressure.

25 Brine content within the Salado is estimated at 1 to 2 percent by weight, although the thin clay
26 seams have been *inferred* observed by Deal et al. (1993, pp. 4-3) to contain up to 25 percent
27 brine by volume. Where sufficient permeability exists, this brine will move towards areas of
28 lower hydraulic potential, such as a borehole or mined section of the Salado.

29 Observation of the response of pore fluids in the Salado to changes in pressure boundary
30 conditions at walls in the repository, in boreholes without packers, in packer-sealed boreholes, or
31 in laboratory experiments is complicated by low permeability and low porosity. Qualitative data
32 on brine flow to underground workings and exploratory boreholes ~~have been~~ *were* collected
33 routinely *between* since 1985 *and 1993* under the Brine Sampling and Evaluation Program
34 (BSEP) and have been documented in a series of reports (Deal and Case 1987; Deal et al. 1987,
35 1989, 1991a, 1991b, and 1993, *and 1995*). ~~These and other investigations are discussed in~~
36 ~~Appendix SUM (Section 3.3.1.3).~~ A discussion of alternative conceptual models for Salado fluid
37 flow is given in Appendix *PA, Attachment* MASS, Section MASS.7. Additional data on brine
38 inflow are available from the Large-Scale Brine Inflow Test (Room Q). Flow has been observed
39 to move to walls in the repository, to boreholes without packers, and to packer-sealed boreholes.
40 These qualitative and relatively short-term observations suggest that brine flow in the fractured
41 DRZ is a complex process. In some locations, evidence for flow is no longer observed where it
42 once was; in others, flow has begun where it once was not observed. In many cases,
43 observations and experiments must last for months or years to obtain useful results.

1 For *PA* modeling, brine flow is a calculated term dependent on local hydraulic gradients and
2 properties of the Salado units. Data on pore pressure and permeability of halite and anhydrite
3 layers are available from the Room Q tests and other borehole tests *as summarized in Beauheim*
4 *and Roberts (2002)*, and these data form the basis for the quantification of the material properties
5 used in the *PA*. See Section 6.4.3.2 for a description of the repository fluid flow model.

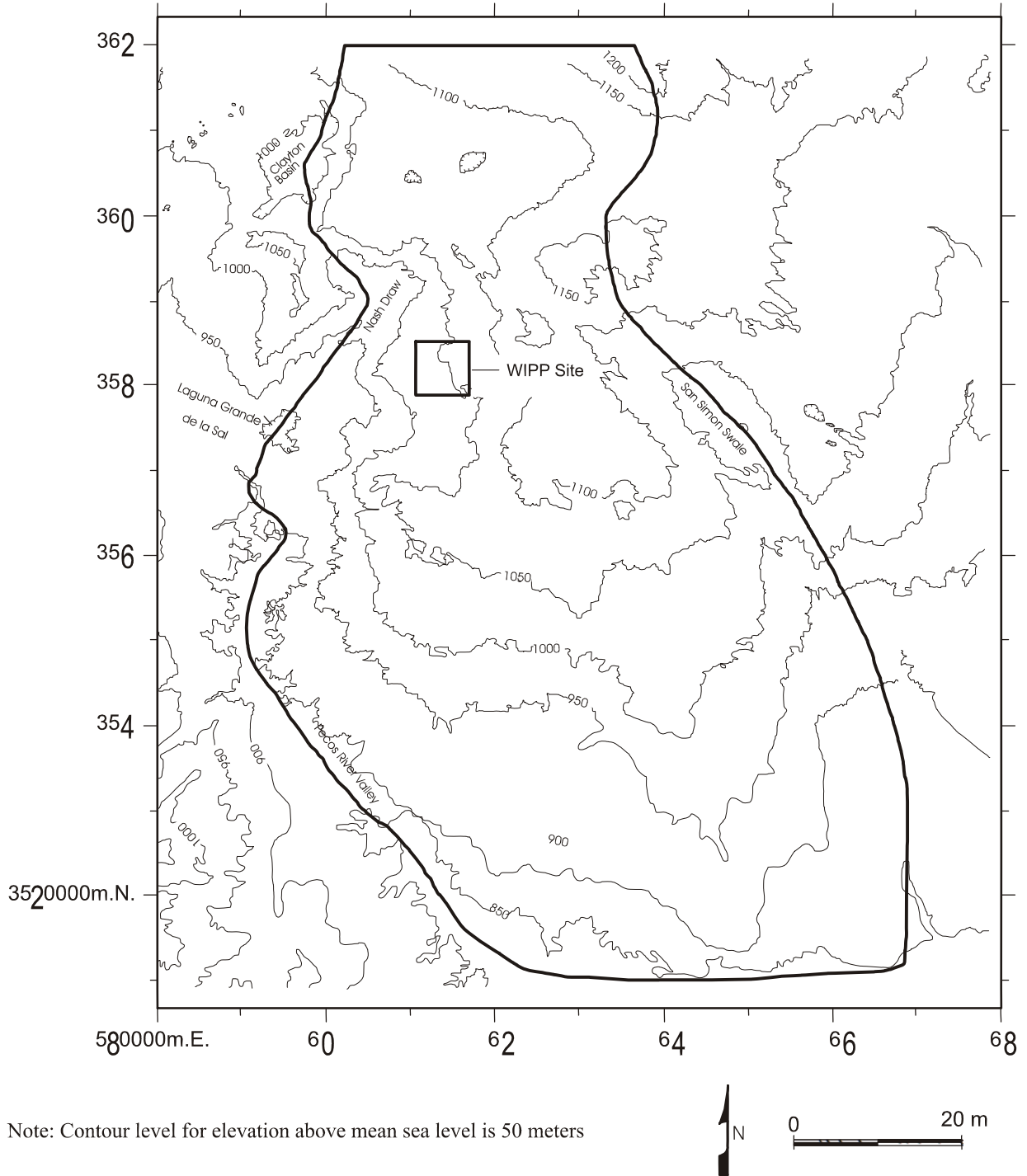
6 Because brine is an important factor in repository performance, several studies of its chemistry
7 have been conducted. Initial investigations were reported in Powers et al. (*CCA* Appendix GCR,
8 Section 7.5) and were continued once access to the underground was established. The most
9 comprehensive data were developed by the BSEP (Deal and Case 1987; Deal et al. 1987, 1989,
10 1991a, 1991b, 1993, *1995*). Results are summarized in Table 2-56. *CCA* Appendix SOTERM
11 discusses the role of brine chemistry in the conceptual model for actinide dissolution. The
12 conceptual model is described in Section 6.4.3.5.

13 2.2.1.4 Units Above the Salado

14 In evaluating groundwater flow above the Salado, the DOE considers the Rustler, Dewey Lake,
15 Santa Rosa, and overlying units to form a groundwater basin with boundaries coinciding with
16 selected groundwater divides as discussed in Section 2.2.1.1. The model boundary follows Nash
17 Draw and the Pecos River valley to the west and south and the San Simon Swale to the east
18 (Figure 2-2933). The boundary continues up drainages and dissects topographic highs along its
19 northern part. These boundaries represent groundwater divides whose positions remain fixed
20 over the past several thousand years and 10,000 years into the future. For reasons described in
21 Section 2.2.1.2.1, the lower boundary of the groundwater basin is the upper surface of the
22 Salado. Nash Draw and the Pecos River are areas where discharge to the surface occurs. Hunter
23 ~~in~~ (1985) described discharge at Surprise Spring and into saline lakes in Nash Draw. She
24 reported groundwater discharge into the Pecos River between Avalon Dam north of Carlsbad and
25 a point south of Malaga Bend as approximately 0.92 m³/sec (32.5 ft³/sec), mostly in the region
26 near Malaga Bend.

27 Within this groundwater basin, hydrostratigraphic units with relatively high permeability are
28 called conductive units, and those with relatively low permeability are called confining layers.
29 The confining layers consist of halite and anhydrite and are perhaps five orders of magnitude less
30 permeable than conductive units.

31 In a groundwater basin, the position of the water table moves up and down in response to
32 changes in recharge. The amount of recharge is generally a very small fraction of the amount of
33 rainfall; this condition is expected for the WIPP. Modeling of recharge changes within the
34 groundwater basin as a function of climate variation is discussed in Section 6.4.9. The water
35 table would stabilize at a particular position if the pattern of recharge remained constant for a
36 long time. The equilibrated position depends, in part, on the distribution of hydraulic
37 conductivity in all hydrostratigraphic units in the groundwater basin. However, the position of
38 the water table depends mainly on the topography and geometry of the groundwater basin and
39 the hydraulic conductivity of the uppermost strata. The position of the water table can adjust
40 slowly to changes in recharge. Consequently, the water table can be at a position that is very
41 much different from its equilibrium position at any given time. Generally, the water table drops



CCA-045-2

1

2 **Figure 2-2933. Outline of the Groundwater Basin Model Domain on a Topographic Map**

3

1 very slowly in response to decreasing recharge but might rise rapidly in times of increasing
2 recharge.

3 The asymmetry of response occurs because the rate at which the water table drops is limited by
4 the rate at which water flows through the entire basin. In contrast, the rate at which the water
5 table rises depends mainly on the recharge rate and the porosity of the uppermost strata. From
6 groundwater basin modeling, the head distribution in the groundwater basin appears to
7 equilibrate rapidly with the position of the water table.

8 The groundwater basin conceptual model (Corbet and Knupp 1996) described above has been
9 implemented in a numerical model, as described in ~~Section 6.4.6.2~~ and **CCA** Appendix MASS,
10 Section MASS.14.2. This model has been used to simulate the interactive nature of flow through
11 conductive layers and confining units for a variety of possible rock properties and climate
12 futures. Thus, this model has allowed insight into the magnitude of flow through various units.
13 The DOE has used this insight as a basis for model simplifications used in **PA** that are described
14 here and in Chapter 6.0.

15 One conclusion from the regional groundwater basin modeling is pertinent here. In general,
16 vertical leakage through confining layers is directed downward over all of the controlled area.
17 This downward leakage uniformly over the WIPP site is the result of a well-developed discharge
18 area, Nash Draw and the Pecos River, along the western and southern boundaries of the
19 groundwater basin. This area acts as a drain for the laterally conductive units in the groundwater
20 basin, causing most vertical leakage in the groundwater basin to occur in a downward direction.
21 This conclusion is important in **PA** simplifications related to the relative importance of lateral
22 flow in the Magenta versus the Culebra, which will be discussed later in this chapter and in
23 Section 6.4.6.

24 *Public concern was expressed that groundwater flow to the spring supplying brine to Laguna*
25 *Grande de la Sal could be related to the presence of karst features. The EPA examined*
26 *information regarding the hydrology of the units above the Salado and DOE's*
27 *conceptualization of the groundwater flow model, including supplementary information*
28 *submitted in letters dated May 2, 1997 (Docket A-93-02, Item V-B-6 (6)), and May 14, 1997*
29 *(Docket A-93-02, Item II-I-31), and the EPA concluded that the information was adequate.*

30 *The EPA concluded, based on WIPP field observations and site-specific hydrologic*
31 *information, there is no indication that any cavernous or other karst-related flow is present*
32 *within the WIPP site boundary. The EPA concurred with DOE's conceptualization of*
33 *groundwater flow in the Culebra, which includes the presence of fractures within the Culebra*
34 *and recharge and discharge areas for groundwater that are more consistent with potential*
35 *discharge to areas south and west of the WIPP.*

36 2.2.1.4.1 Hydrology of the Rustler Formation

37 The Rustler is of particular importance for WIPP because it contains the most transmissive units
38 above the repository. Fluid flow in the Rustler is characterized by very slow rates of vertical
39 leakage through confining layers and faster lateral flow in conductive units. To illustrate this
40 point, regional modeling with the groundwater basin model indicates that lateral specific

1 discharges in the Culebra, for example, are perhaps two to three orders of magnitude greater than
2 the vertical specific discharges across the top of the Culebra.

3 *Because of its importance, the Rustler continues to be the focus of studies to understand better*
4 *the complex relationship between hydrologic properties and geology, particularly in view of*
5 *water-level rises observed in the Culebra and Magenta (e.g., SNL 2003a; also see Appendix*
6 *DATA). An example of the complex nature of Rustler hydrology is the variation in Culebra*
7 *transmissivity (T). Culebra T varies over three orders of magnitude on the WIPP site itself*
8 *and over six orders of magnitude on the scale of the regional groundwater basin model with*
9 *lower T east of the site and higher T west of the site in Nash Draw (e.g., Beauheim and*
10 *Ruskauff 1998). As discussed below, site investigations and studies (e.g., Holt and Powers*
11 *1988; Beauheim and Holt 1990; Powers and Holt 1995; Holt 1997; Holt and Yarbrough 2002;*
12 *Powers et al. 2003) suggest that the variability in Culebra T can be explained largely by the*
13 *thickness of Culebra overburden, the location and extent of upper Salado dissolution, and the*
14 *occurrence of halite in the mudstone units bounding the Culebra (see Section 2.1.3.5).*

15 2.2.1.4.1.1 ~~Unnamed Lower Member~~ *Los Medaños*

16 *The unnamed lower member was named the Los Medaños by Powers and Holt (1999).* ~~The~~
17 ~~unnamed lower member makes up~~ *The Los Medaños is treated as* a single hydrostratigraphic
18 unit in WIPP models of the Rustler, although its composition varies. Overall, it acts as a
19 confining layer. The basal interval of the *Los Medaños* ~~unnamed lower member~~, approximately
20 19.5 m (64 ft) thick, is composed of siltstone, mudstone, and claystone and contains the water-
21 producing zones of the lowermost Rustler. Transmissivities of 2.9×10^{-10} m²/see (2.7×10^{-4}
22 ft²/day) and 2.4×10^{-10} m²/see (2.2×10^{-4} ft²/day) were reported by Beauheim (1987a, p. 50)
23 from tests at well H-16 that included this interval. The porosity of the ~~unnamed lower member~~
24 *Los Medaños* was measured in 1995 as part of testing at the H-19 hydropad (*TerraTek 1996*).
25 Two claystone samples had effective porosities of 26.8 and 27.3 percent. One anhydrite sample
26 had an effective porosity of 0.2 percent. The transmissivity values correspond to hydraulic
27 conductivities of 1.5×10^{-11} m/see (4.2×10^{-6} ft/day) and 1.2×10^{-11} m/see (3.4×10^{-6} ft/day).
28 Hydraulic conductivity in the lower portion of the ~~unnamed lower member~~ *Los Medaños* is
29 believed by the DOE to increase to the west in and near Nash Draw, where dissolution at the
30 underlying Rustler-Salado contact has caused subsidence and fracturing of the sandstone and
31 siltstone.

32 The remainder of the *Los Medaños* ~~unnamed lower member~~ contains mudstones, anhydrite, and
33 variable amounts of halite. The hydraulic conductivity of these lithologies is extremely low. It
34 is for this reason the *Los Medaños* ~~unnamed lower member~~ is treated as a single
35 hydrostratigraphic unit that overall acts as a confining unit. The conceptual model incorporating
36 the ~~unnamed lower member~~ *Los Medaños* is discussed in Section 6.4.6.1. Important hydrologic
37 model properties of the ~~unnamed lower member~~ are discussed in Section 6.4.6.1 and are
38 summarized in Appendix PAR (Table PAR-31). *of the Los Medaños are summarized in*
39 *Appendix PA.*

40 *As described in Section 2.1.3.5, the Los Medaños contains two mudstone layers: one in the*
41 *middle of the Los Medaños and one immediately below the Culebra. An anhydrite layer*
42 *separates the two mudstones. The lower and upper Los Medaños mudstones have been given*

1 *the designations M1/H1 and M2/H2, respectively, by Holt and Powers (1988). This naming*
 2 *convention is used to indicate the presence of halite in the mudstone at some locations at and*
 3 *near the WIPP site. Powers (2002a) has mapped (Figure 2-15) the margins delineating the*
 4 *occurrence of halite in both mudstone layers. Whereas early researchers (e.g., Snyder 1985)*
 5 *interpreted the absence of halite west of these margins as evidence of dissolution, Holt and*
 6 *Powers (1988) interpreted it as reflecting changes in the depositional environment, not*
 7 *dissolution. However, Holt and Powers (1988) concluded that dissolution of Rustler halite*
 8 *may have occurred along the present-day margins. The presence of halite in the Los Medaños*
 9 *mudstones is likely to affect the conductivity of the mudstones, but its greater importance is the*
 10 *implications it has for the conductivity of the Culebra. As discussed in Section 2.2.1.4.1.2, the*
 11 *Culebra transmissivity in locations where halite is present in M2/H2 and M3/H3 (a mudstone*
 12 *in the lower Tamarisk Member of the Rustler) is assumed to be an order of magnitude lower*
 13 *than where halite does not occur (Holt and Yarbrough 2002).*

14 *Fluid pressures in the Los Medaños have been continuously measured at well H-16 since*
 15 *1987. During this period, the fluid pressure has remained relatively constant at between 190*
 16 *and 195 psi or a head of approximately 137 m (450 ft). Given the location of the pressure*
 17 *transducer (an elevation of 811.96 m amsl), the current elevation of the Los Medaños water*
 18 *level at H-16 is approximately 949 m amsl. No other wells in the WIPP monitoring network*
 19 *are completed to the Los Medaños. Thus, H-16 provides the only current head information*
 20 *for this member.*

21 2.2.1.4.1.2 The Culebra *Dolomite Member*

22 The Culebra is of interest because it is the most transmissive *saturated* unit *above* at the WIPP
 23 *repository* site and hydrologic research has been concentrated on the unit for *nearly two* over a
 24 decades. Although it is relatively thin, it is an entire hydrostratigraphic unit in the WIPP
 25 hydrological conceptual model, and it is the most important conductive unit in this model.
 26 Implementation of the Culebra in the conceptual model is discussed in detail in Section 6.4.6.2.
 27 Model discussions cover groundwater flow and transport characteristics of the Culebra. These
 28 are supported by parameter values in Table 6-20, 6-21, 6-22, and 6-23. Additional background
 29 for the Culebra model is in *CCA* Appendix MASS, Sections MASS.14 and MASS.15.

30 The two primary types of field tests ~~that are being~~ used to characterize the flow and transport
 31 characteristics of the Culebra are hydraulic tests and tracer tests.

32 The hydraulic testing consists of pumping, injection, and slug testing of wells across the study
 33 area (for example, Beauheim 1987a, *p.* 3). The most detailed hydraulic test data exist for the
 34 WIPP hydropads (for example, H-19). The hydropads generally comprise a network of three or
 35 more wells located within a few tens of meters of each other. Long-term pumping tests have
 36 been conducted at hydropads H-3, H-11, and H-19 and at well WIPP-13 (Beauheim 1987b;
 37 1987c; 1989; Beauheim et al. 1995; *Meigs et al. 2000*). These pumping tests provided transient
 38 pressure data at the hydropad and over a much larger area. Tests often included use of
 39 automated data-acquisition systems, providing high-resolution (in both space and time) data sets.
 40 In addition to long-term pumping tests, slug tests and short-term pumping tests have been
 41 conducted at individual wells to provide pressure data that can be used to interpret the
 42 transmissivity at that well (Beauheim 1987a). (Additional short-term pumping tests have been

1 conducted in the WQSP wells [*Beauheim and Ruskauff 1998* ~~Stensrud 1995~~]. Detailed cross-
2 hole hydraulic testing has recently been conducted at the H-19 hydropad (*Kloska et al.*
3 ~~1995~~ *Beauheim 2000*).

4 The hydraulic tests are designed to yield pressure data for the interpretation of such
5 characteristics as transmissivity, permeability, and storativity. The pressure data from long-term
6 pumping tests and the interpreted transmissivity values for individual wells are used for the
7 generation of transmissivity fields in *PA* flow modeling (see Appendix *PA, Attachment*
8 *TFIELD*, Sections *TFIELD-2 5.0 and TFIELD-6.0*). Some of the hydraulic test data and
9 interpretations are also important for the interpretation of transport characteristics. For instance,
10 information about the vertical distribution of the permeability values interpreted from the
11 hydraulic tests at a given hydropad ~~are~~ *is* needed for interpretations of tracer test data at that
12 hydropad.

13 To evaluate transport properties of the Culebra, a series of tracer tests ~~has been~~ *were* conducted
14 at six locations (the H-2, H-3, H-4, H-6, H-11, and H-19 hydropads) near the WIPP site. Tests at
15 the first five of these locations consisted of two-well dipole tests and/or multiwell convergent
16 flow tests and are described in detail in Jones et al. (1992). Tracer tests at the H-19 hydropad
17 and additional tracer tests performed at the H-11 hydropad are described in ~~Beauheim et al.~~
18 ~~(1995)~~ *Meigs et al. (2000)*. The ~~more recent~~ *1995-1996* tracer test program consisted of single-
19 well injection-withdrawal tests and multi-well convergent flow tests (*Meigs and Beauheim*
20 *2001*). Unique features of this testing program include the single-well test at both H-19 and H-
21 11, the injection of tracers into six wells during the H-19 convergent-flow test, the injection of
22 tracer into upper and lower zones of the Culebra at the H-19 hydropad, repeated injections under
23 different convergent-flow pumping rates, and the use of tracers with different free-water
24 diffusion coefficients. The *1995-1996* ~~recent~~ tracer tests were specifically designed to evaluate
25 the importance of heterogeneity (both horizontal and vertical) and diffusion on transport
26 processes.

27 The Culebra is a fractured dolomite with nonuniform properties both horizontally and vertically.
28 Examination of core and shaft exposures has revealed that there are multiple scales of porosity
29 within the Culebra including fractures ranging from microscale to potentially large, vuggy zones,
30 and interparticle and intercrystalline porosity (*Holt 1997*). Porosity measurements made on core
31 samples give porosity measurements ranging from 0.03 to 0.30 (Kelley and Saulnier 1990;
32 *TerraTek 1996*). This large range in porosity for small samples is expected given the variety of
33 porosity types within the Culebra. However, the effective porosity for flow and transport at
34 larger scales will have a smaller range due to the effects of spatial averaging. The core
35 measurements indicate that the Culebra has significant quantities of connected porosity.

36 Flow in the Culebra occurs within fractures, within vugs where they are connected by fractures,
37 and to some extent within interparticle porosity where the porosity (and permeability) is high,
38 such as chalky lenses. At any given location, flow will occur in response to hydraulic gradients
39 in all places that are permeable. When the permeability contrast between different scales of
40 connected porosity is large, the total porosity can effectively be conceptualized by dividing the
41 system into advective porosity (often referred to as fracture porosity) and diffusive porosity
42 (often referred to as matrix porosity). The advective porosity can be defined as the portion of the
43 porosity where flow is the dominant process (for example fractures and to some extent vugs

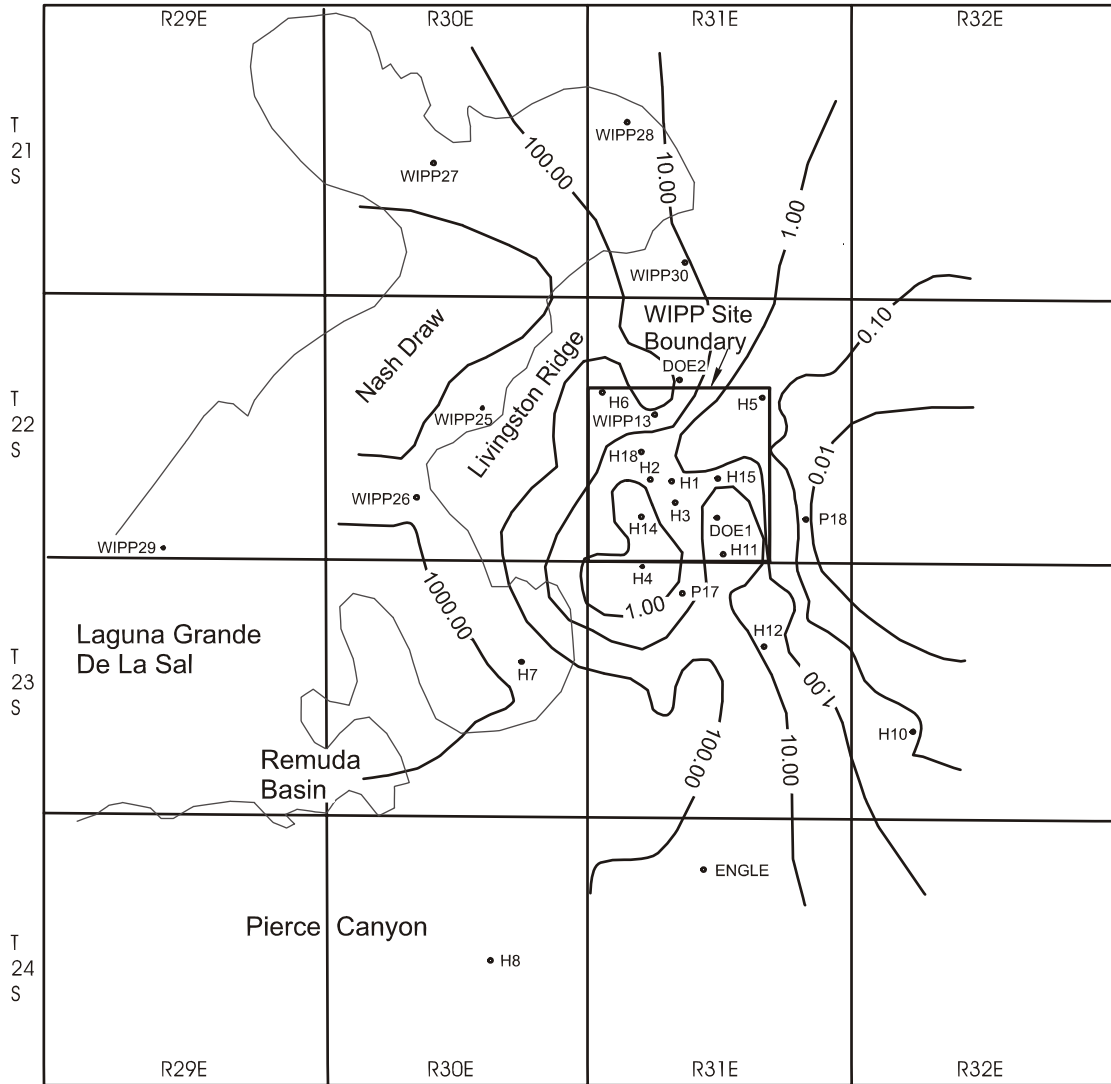
1 connected by fractures and interparticle porosity). Diffusive porosity can be defined as the
2 portion of the porosity where diffusion is the dominant process (for example, intercrystalline
3 porosity and to some extent microfractures, vugs and portions of the interparticle porosity.)

4 For the Culebra in the vicinity of the WIPP site, defining advective porosity is not a simple
5 matter. In some regions the permeability of the fractures is inferred to be significantly larger
6 than the permeability of the other porosity types, thus advective porosity can be conceptualized
7 as predominantly fracture porosity (low porosity). In some regions, there appear to be no high
8 permeability fractures. This may be due to a lack of large fractures or may be the result of
9 gypsum fillings in a portion of the porosity. Where permeability contrasts between porosity
10 types are small, the advective porosity can be conceptualized as a combination of fractures, vugs
11 connected by fractures, and permeable portions of the interparticle porosity. In each case, the
12 diffusive porosity can be conceptualized as the porosity where advection is not dominant.

13 The major physical transport processes that affect actinide transport through the Culebra include
14 advection (through fractures and other permeable porosity), diffusion from the advective porosity
15 into the rest of the connected porosity (diffusive porosity) and dispersive spreading due to
16 heterogeneity. Diffusion can be an important process for effectively retarding solutes by
17 transferring mass from the porosity where advection (flow) is the dominant process into other
18 portions of the rock. Diffusion into stagnant portions of the rock also provides access to
19 additional surface area for sorption. ~~A further discussion of transport of actinides in the~~
20 Culebra as either dissolved species or as colloids is given in Section 6.4.6.2. Parameter values
21 determined from tests of the Culebra are given in *CCA* Appendix PAR and are described in
22 Section 6.4.6.2.2. A summary of input values to the conceptual model ~~is~~ are in Tables 6-22 and
23 6-23.

24 Fluid flow in the Culebra is dominantly lateral and southward except in discharge areas along the
25 west or south boundaries of the basin. Where transmissive fractures exist, flow is dominated by
26 fractures but may also occur in vugs connected by microfractures and interparticle porosity.
27 Regions where flow is dominantly through vugs connected by microfractures and interparticle
28 porosity have been inferred from pumping tests and tracer tests. Flow in the Culebra may be
29 concentrated along zones that are thinner than the total thickness of the Culebra. In general, the
30 upper portion of the Culebra is massive dolomite with a few fractures and vugs, and appears to
31 have low permeability. The lower portion of the Culebra appears to have many more vuggy and
32 fractured zones and to have a significantly higher permeability (Meigs and Beauheim 2001).

33 There is strong evidence that the permeability of the Culebra varies spatially and varies
34 sufficiently that it cannot be characterized with a uniform value or range over the region of
35 interest to the WIPP. The transmissivity of the Culebra varies spatially over six orders of
36 magnitude from east to west in the vicinity of the WIPP (Figure 2-30~~34~~). Over the site, Culebra
37 transmissivity varies over three to four orders of magnitude. *CCA* Appendix TFIELD, Section
38 TFIELD.2 contains the data used to develop Figure 2-30~~34~~, which shows variation in
39 transmissivity in the Culebra in the WIPP region. *Attachment TFIELD to Appendix*
40 *PA* Appendix MASS (Section MASS.15, including MASS Attachment 15-6) provides *the*
41 modeling rationale and. ~~The discussion in Appendix TFIELD~~ addresses how data collected over
42 a number of years were correlated for the generations of transmissivity fields.



• Observation Well



Note: Transmissivities are given in square feet per day. Figure is modified from Cauffman et al. 1990 (Figure 5.22a). See Appendix TFIELD for details of the performance assessment implementation.

CCA-046-2

1

2

Figure 2-3034. Transmissivities of the Culebra

3 Transmissivities are from about 1×10^{-9} m²/sec (1×10^{-3} ft²/day) at well P-18 east of the WIPP
 4 site to about 1×10^{-3} m²/sec (1×10^3 ft²/day) at well H-7 in Nash Draw (see Figure 2-2 for the
 5 locations of these wells and see Figure 4-8 in CCA Appendix FAC for a Culebra isopach map).

6 Transmissivity variations in the Culebra are believed to be controlled by the relative abundance
 7 of open fractures rather than by primary (that is, depositional) features of the unit. Lateral

1 variations in depositional environments were small within the mapped region, and primary
 2 features of the Culebra show little map-scale spatial variability, according to Holt and Powers
 3 (CCA Appendix FAC). Direct measurements of the density of open fractures are not available
 4 from core samples because of incomplete recovery and fracturing during drilling, but observation
 5 of the relatively unfractured exposures in the WIPP shafts suggests that the density of open
 6 fractures in the Culebra decreases to the east. Qualitative correlations have been noted between
 7 transmissivity and several geologic features possibly related to open fracture density, including
 8 (1) the distribution of overburden above the Culebra, (2) the distribution of halite in other
 9 members of the Rustler, (3) the dissolution of halite in the upper portion of the Salado, and
 10 (4) the distribution of gypsum fillings in fractures in the Culebra (see Section 2.1.3.5.2 and
 11 Figure 2-12).

12 *Recent investigations have made a significant contribution to the understanding of the large*
 13 *variability observed for Culebra transmissivity (e.g., Holt and Powers 1988; Beauheim and*
 14 *Holt 1990; Powers and Holt 1995; Holt 1997; Holt and Yarbrough 2002; Powers et al. 2003).*
 15 *The spatial distribution of Culebra transmissivity is believed to be due strictly to deterministic*
 16 *post-depositional processes and geologic controls (Holt and Yarbrough 2002). The important*
 17 *geologic controls include Culebra overburden thickness, dissolution of the upper Salado, and*
 18 *the occurrence of halite in the mudstone Rustler units (M2/H2 and M3/H3) above and below*
 19 *the Culebra (Holt and Yarbrough 2002). Culebra transmissivity is inversely related to*
 20 *thickness of overburden because stress relief associated with erosion of overburden (see*
 21 *Section 2.1.5.2) leads to fracturing and opening of preexisting fractures. Culebra*
 22 *transmissivity is high where dissolution of the upper Salado has occurred and the Culebra has*
 23 *subsided and fractured. Culebra transmissivity is observed to be low where halite is present in*
 24 *overlying and/or underlying mudstones. Presumably, high Culebra transmissivity leads to*
 25 *dissolution of nearby halite (if any). Hence, the presence of halite in mudstones above and/or*
 26 *below the Culebra can be taken as an indicator for low Culebra transmissivity. Details of the*
 27 *geologic-based transmissivity model for the Culebra are given in Attachment TFIELD*
 28 *(Section TFIELD-3.0) to Appendix PA and summarized below.*

29 *The Culebra has been tested hydraulically at 42 locations, yielding reliable transmissivity*
 30 *values. These values (log T) are plotted as a function of depth to Culebra (overburden*
 31 *thickness) in Figure 2-35. As shown, the Culebra transmissivities fall into two populations*
 32 *separated by a cutoff (termed 'high-T' cutoff) equal to -5.4 (log T [m²/s]). These data suggest*
 33 *a bimodal distribution for transmissivity with one population having high transmissivity and*
 34 *the other low transmissivity, with the difference attributed to open, interconnected fractures*
 35 *("fracture interconnectivity") for the high-transmissivity population (Holt and Yarbrough*
 36 *2002). Using these data, Holt and Yarbrough (2002) constructed a linear Culebra*
 37 *transmissivity model relating log T to the deterministic geologic controls described above. The*
 38 *linear model is expressed as follows:*

$$39 \quad Y(\mathbf{x}) = \beta_1 + \beta_2 d(\mathbf{x}) + \beta_3 I_f(\mathbf{x}) + \beta_4 I_D(\mathbf{x}), \quad (2.1)$$

40 *where Y(x) is log T (x), β_i (i = 1 to 4) are regression coefficients, x is a two-dimensional*
 41 *location vector, d(x) is the overburden thickness at x (expressed in UTM coordinates and*

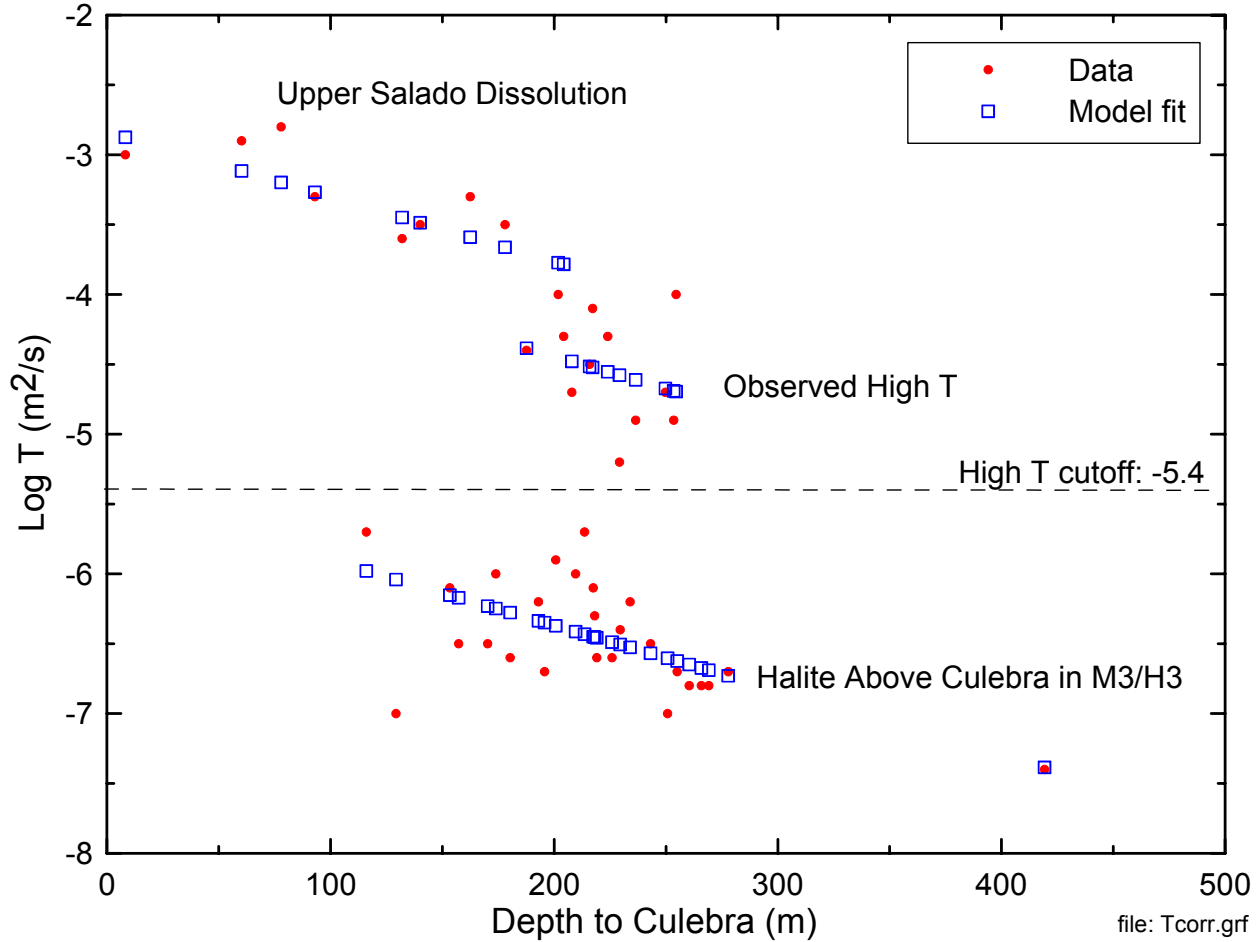


Figure 2-35. Correlation Between Culebra Transmissivity ($\log T$ (m^2/s)) and Overburden Thickness for Different Geologic Environments (after Holt and Yarbrough 2002)

meters), $I_f(x)$ is the fracture-interconnectivity indicator at x (equal to 1 when $\log T$ (m^2/s) > -5.4 or 0 when $\log T$ (m^2/s) < -5.4), and $I_D(x)$ is the dissolution indicator (equal to 1 when Salado dissolution has occurred at (x) and 0 when it has not). In this model, coefficient β_1 is the intercept value, β_2 is the slope of $Y(x)/d(x)$, and β_3 and β_4 represent adjustments to the intercept for the occurrence of open, interconnected fractures and Salado dissolution, respectively. Based on linear-regression analysis, Holt and Yarbrough (2002) estimated the coefficients in Equation (2.1). These estimates are summarized in Table 2-7. Predictions of the Culebra transmissivity model represented by Equation (2.1) are shown in Figure 2-35.

The regression model expressed by Equation (2.1) cannot adequately predict transmissivity in the regions where halite is present both in M2/H2 and M3/H3. In these regions, Culebra

Table 2-7. Estimates of Culebra Transmissivity Model Coefficients

β_1	β_2	β_3	β_4
-5.441	-4.636×10^{-3}	1.926	0.678

1 *porosity is thought to be at least partially filled with halite, reducing transmissivity. For these*
 2 *regions, Equation (2.1) is modified as follows:*

$$3 \quad Y(\mathbf{x}) = \beta_1 + \beta_2 d(\mathbf{x}) + \beta_3 I_f(\mathbf{x}) + \beta_4 I_D(\mathbf{x}) + \beta_5 I_H(\mathbf{x}). \quad (2.2)$$

4 *$I_H(x)$ is a halite indicator function equal to 1 in locations where halite occurs in both the*
 5 *M2/H2 and M3/H3 intervals and 0 otherwise. The coefficient β_5 is equal to -1 to assure that*
 6 *the model in Equation (2.2) reduces the predicted transmissivity values by one order of*
 7 *magnitude where halite occurs in both the M2/H2 and M3/H3 intervals.*

8 *In the region east of the upper Salado dissolution margin and west of the M2/H2 and M3/H3*
 9 *margins, high transmissivity depends, in part, on the absence of gypsum fracture fillings. No*
 10 *method has yet been determined for predicting whether fractures will or will not be filled with*
 11 *gypsum at a given location, so the distribution of high and low transmissivity is treated*
 12 *stochastically in this region. Predictions of transmissivity in this region make use of an*
 13 *isotropic spherical variogram model. Fitted parameters for the variogram model are described*
 14 *in Attachment TFIELD (Section TFIELD-4.3) of Appendix PA.*

15 Geochemical and radioisotope characteristics of the Culebra have been studied. There is
 16 considerable variation in groundwater geochemistry in the Culebra. The variation has been
 17 described in terms of different hydrogeochemical facies that can be mapped in the Culebra (see
 18 Section 2.4.2). A halite-rich hydrogeochemical facies exists in the region of the WIPP site and
 19 to the east, approximately corresponding to the regions in which halite exists in units above and
 20 below the Culebra (Figure 2-10) (Figure 2-15), and in which a large portion of the Culebra
 21 fractures are gypsum filled (Figure 2-12, 17). An anhydrite-rich hydrogeochemical facies exists
 22 west and south of the WIPP site, where there is relatively less halite in adjacent strata and where
 23 there are fewer gypsum-filled fractures.

24 *The Culebra groundwater geochemistry studies continue. Culebra water quality is evaluated*
 25 *semiannually at six wells, three north (WQSP-1, WQSP-2, and WQSP-3) and three south*
 26 *(WQSP-4, WQSP-5, and WQSP-6) (WIPP MOC 1995) of the surface structures area (see*
 27 *Figure 2-3 for well locations). Five rounds of semiannual sampling of water quality*
 28 *completed before the first receipt of waste at the WIPP were used to establish the initial*
 29 *Culebra water-quality baseline for major ion species including Na^+ , Ca^{2+} , Mg^{2+} , K^+ , Cl^- ,*
 30 *SO_4^{2-} , and HCO_3^{2-} (Crawley and Nagy 1998). In 2000, this baseline was expanded to include*
 31 *five additional rounds of sampling that were completed before first receipt of RCRA-regulated*
 32 *waste (IT Corporation 2000). Table 2-8 gives the 95 percent confidence intervals presented in*
 33 *SNL (2001) for the major ion species determined from the 10 rounds (semiannual sampling*
 34 *for 5 years) of baseline sampling. Culebra water quality is extremely variable among the six*
 35 *sampling wells, as shown by the Cl^- concentrations that range from approximately 6,000 mg/L*
 36 *at WQSP-6 to 130,000 mg/L at WQSP-3.*

37 Radiogenic isotopic signatures suggest that the age of the groundwater in the Culebra is on the
 38 order of 10,000 years or more (see, for example, Lambert 1987, Lambert and Carter 1987, and
 39 Lambert and Harvey 1987 in the bibliography). The radiogenic ages of the Culebra groundwater
 40 and the geochemical differences provide information potentially relevant to the groundwater
 41 flow directions and groundwater interaction with other units and are important constraints on

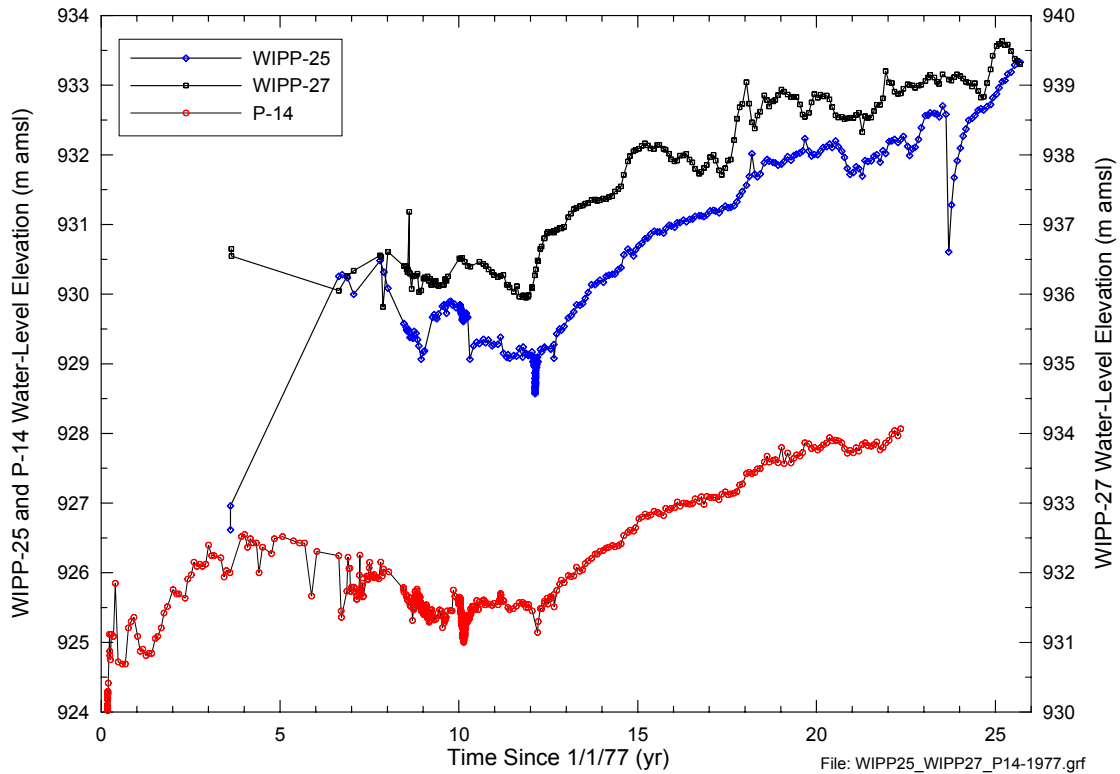
1 **Table 2-8. Ninety-Five Percent Confidence Intervals for Culebra Water-Quality Baseline**

<i>Well I.D.</i>	<i>Cl Conc. (mg/L)</i>	<i>SO₄²⁻ Conc. (mg/L)</i>	<i>HCO₃⁻ Conc. (mg/L)</i>	<i>Na⁺ Conc. (mg/L)</i>	<i>Ca²⁺ Conc. (mg/L)</i>	<i>Mg²⁺ Conc. (mg/L)</i>	<i>K⁺ Conc. (mg/L)</i>
<i>WQSP-1</i>	<i>31100-39600</i>	<i>4060-5600</i>	<i>45-54</i>	<i>15850-21130</i>	<i>1380-2030</i>	<i>940-1210</i>	<i>322-730</i>
<i>WQSP-2</i>	<i>31800-39000</i>	<i>4550-6380</i>	<i>43-53</i>	<i>14060-22350</i>	<i>1230-1730</i>	<i>852-1120</i>	<i>318-649</i>
<i>WQSP-3</i>	<i>113900-145200</i>	<i>6420-7870</i>	<i>23-51</i>	<i>62600-82700</i>	<i>1090-1620</i>	<i>1730-2500</i>	<i>2060-3150</i>
<i>WQSP-4</i>	<i>53400-63000</i>	<i>5620-7720</i>	<i>31-46</i>	<i>28100-37800</i>	<i>1420-1790</i>	<i>973-1410</i>	<i>784-1600</i>
<i>WQSP-5</i>	<i>13400-17600</i>	<i>4060-5940</i>	<i>42-54</i>	<i>7980-10420</i>	<i>902-1180</i>	<i>389-535</i>	<i>171-523</i>
<i>WQSP-6</i>	<i>5470-6380</i>	<i>4240-5120</i>	<i>41-54</i>	<i>3610-5380</i>	<i>586-777</i>	<i>189-233</i>	<i>113-245</i>

2 conceptual models of groundwater flow. Previous conceptual models of the Culebra (see for
 3 example, Chapman 1986, Chapman 1988, LaVenue et al. 1990, and Siegel et al. 1991 ~~in the~~
 4 ~~bibliography~~) have not been able to consistently relate the hydrogeochemical facies, radiogenic
 5 ages, and flow constraints (that is, transmissivity, boundary conditions, etc.) in the Culebra.

6 The groundwater basin modeling that ~~has been~~ **was** conducted, although it did not model solute
 7 transport processes, provides flow fields that can be used to develop the following concepts that
 8 help explain the observed hydrogeochemical facies and radiogenic ages. The groundwater basin
 9 model combines and tests three fundamental processes: (1) it calculates vertical leakage, which
 10 may carry solutes into the Culebra; (2) it calculates lateral fluxes in the Culebra (directions as
 11 well as rates); and (3) it calculates a range of possible effects of climate change. The presence of
 12 the halite-rich groundwater facies is explained by vertical leakage of solutes into the Culebra
 13 from the overlying halite-containing Tamarisk by advective or diffusive processes. Because
 14 lateral flow rates here are low, even slow rates of solute transport into the Culebra can result in
 15 high solute concentration. Vertical leakage occurs slowly over the entire model region, and thus
 16 the age of groundwater in the Culebra is old, consistent with radiogenic information. Lateral
 17 fluxes within the anhydrite zone are larger because of higher transmissivity, and where the halite
 18 and anhydrite facies regions converge, the halite facies signature is lost by dilution with
 19 relatively large quantities of anhydrite facies groundwater. Response of groundwater flow in the
 20 Culebra as the result of increasing recharge is modeled through the variation in climate,
 21 discussed in Section 6.4.9.

22 Groundwater levels in the Culebra in the WIPP region ~~have been~~ **were** measured continuously
 23 **prior to** ~~for several decades~~ **the CCA in numerous wells (Figure 2-2)**. Water level rises have
 24 been observed in the WIPP region and are attributed to three causes as discussed below. The
 25 extent of water level rise observed at a particular well depends on several factors, but the
 26 proximity of the observation point to the cause of the water level rise appears to be a primary
 27 factor. **The Culebra monitoring wells as of the end of 2002 are shown in Figures 2-3 and 2-4;**
 28 **plugged and abandoned wells are not shown in these figures. Beginning in 1989, a general**



1
2 **Figure 2-36. Water-level Trends in Nash Draw Wells and at P-14 (see Figure 2-2 for well**
3 **locations)**

4 *long-term rise has been observed in both Culebra and Magenta water levels (Figure 2-36) over*
5 *a broad area of the WIPP site including Nash Draw (SNL 2003a). At the time of the CCA this*
6 *long-term rise was recognized, but was thought (outside of Nash Draw) to represent recovery*
7 *from the accumulation of hydraulic tests that had occurred since the late 1970s and the effects*
8 *of grouting around the WIPP shafts to limit leakage. Water levels in Nash Draw were thought*
9 *to respond to changes in the volumes of potash mill effluent discharged into the draw (Silva*
10 *1996); however, correlation of these water levels with potash mine discharge cannot be proven*
11 *because sufficient data on the timing and volumes of discharge are not available. As the rise*
12 *in water levels has continued since 1996, observed heads have exceeded the ranges of*
13 *uncertainty established for the steady-state heads in most of the 32 wells used in the*
14 *calibration of the transmissivity fields described in CCA Appendix TFIELD. Although*
15 *recovery from the hydraulic tests and shaft leakage has unquestionably occurred, the DOE*
16 *has implemented a program to identify other potential causes for the water-level rises (SNL*
17 *2003b).*

18 ~~In the vicinity of the WIPP site, water level rises are unquestionably caused by recovery from~~
19 ~~drainage into the shafts. Drainage into shafts has been reduced by a number of grouting~~
20 ~~programs over the years, most recently in 1993 around the AIS. Northwest of the site, in and~~
21 ~~near Nash Draw, water levels appear to fluctuate in response to effluent discharge from potash~~
22 ~~mines. Correlation of water level fluctuation with potash mine discharge cannot be proven~~
23 ~~because sufficient data on the timing and volumes of discharge are not available.~~

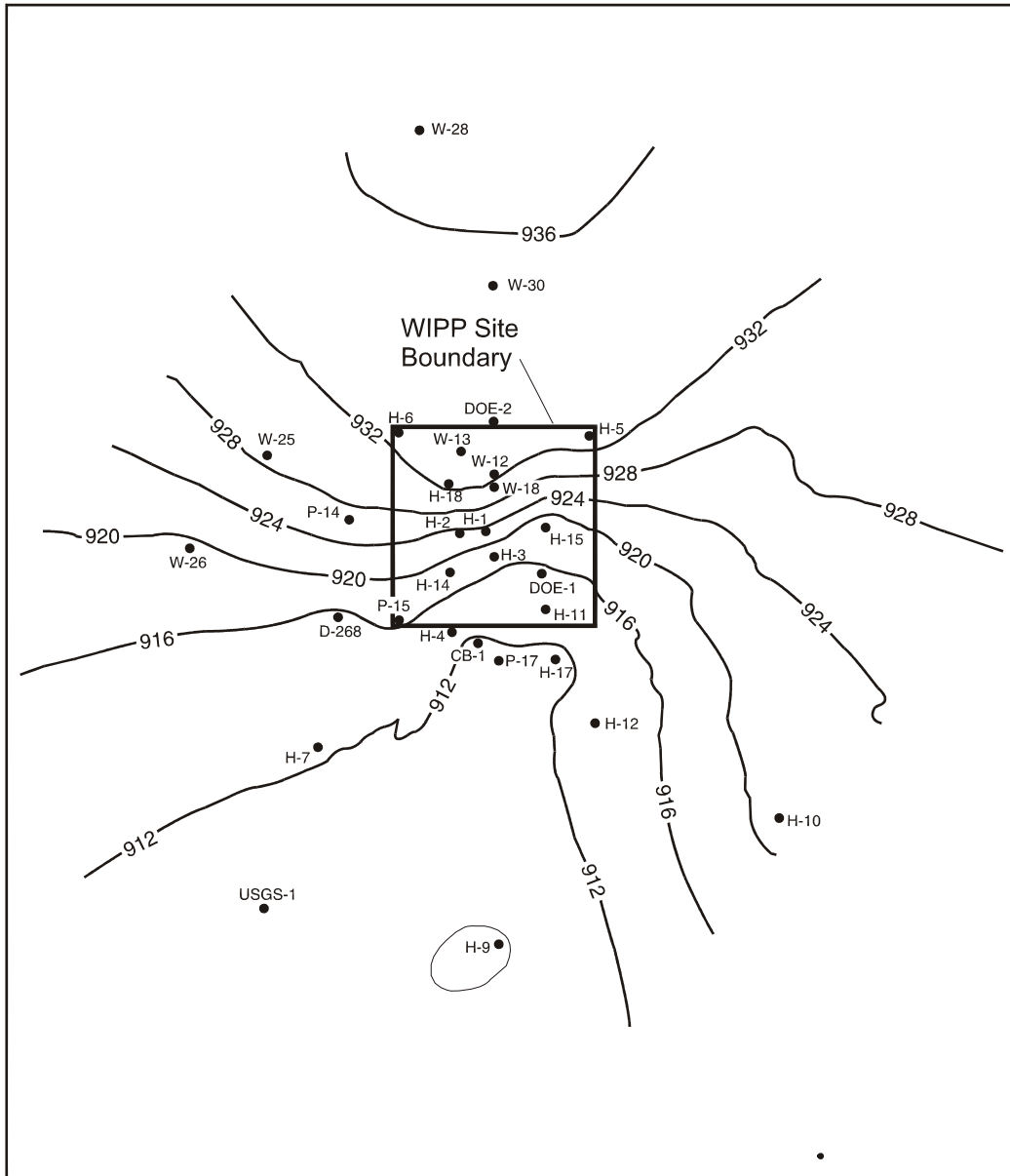
1 *Although Culebra heads have been rising, the head* Head distribution in the Culebra (see
 2 *Figure 2-31) (see Figure 2-37)* is consistent with groundwater basin modeling results (discussed
 3 in Section 6.4.6 and Appendix *PA, Attachment MASS*, Section MASS.14.2) indicating that the
 4 generalized direction of groundwater flow *remains* north to south. However, caution should be
 5 used when making assumptions based on groundwater-level data alone. Studies in the Culebra
 6 have shown that fluid density variations in the Culebra can affect flow direction (Davies 1989, p.
 7 35). The fractured nature of the Culebra, coupled with variable fluid densities, can also cause
 8 localized flow patterns to differ from general flow patterns. Water-level rises in the vicinity of
 9 the H-9 hydrograd, about 10.46 km (6.5 mi) south of the site, are not thought to be caused by
 10 either WIPP activities or potash mining discharge *and have been included in the DOE program*
 11 *to investigate Culebra water-level rises in general.* They remain unexplained. The DOE
 12 continues to monitor groundwater levels throughout the region, but only water-level changes at
 13 or near the site have the potential to affect performance *impact the prediction of disposal system*
 14 *performance.* The DOE has implemented water-level changes in its conceptual model through
 15 variations in climate as discussed in Section 6.4.9. These variations bring the water level *table* to
 16 the surface for some calculations. This modeling simplification bounds the possible effects of
 17 anomalous water level changes regardless of their origin. *The DOE has also used recent (late*
 18 *2000) Culebra heads in flow and transport calculations for this recertification application, as*
 19 *discussed in Appendix PA, Attachment TFIELD, Section TFIELD-6.2.*

20 Inferences about vertical flow directions in the Culebra have been made from well data collected
 21 by the DOE. Beauheim (1987a) reported flow directions towards the Culebra from both the
 22 ~~unnamed lower member~~ *Los Medaños* and the Magenta over the WIPP site, indicating that the
 23 Culebra acts as a drain for the units around it. This indication is consistent with results of
 24 groundwater basin modeling. A more detailed discussion of Culebra flow and transport can be
 25 found in *Appendix PA, Attachment TFIELD* Appendices (MASS [(Sections MASS.14 and
 26 MASS.15)] and TFIELD).

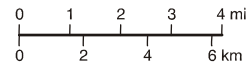
27 *In response to an EPA letter dated March 19, 1997 (Docket A-93-02, Item II-I-17),*
 28 *supplemental information to the CCA pertinent to groundwater flow and geochemistry within*
 29 *the Culebra was provided by the DOE in a letter dated May 14, 1997 (Docket A-93-02, Item II-*
 30 *I-31). In that letter, the DOE explained the conceptual model of Culebra groundwater flow*
 31 *used in the CCA. The CCA conceptual model, referred to as the groundwater basin model,*
 32 *offers a three-dimensional approach to treatment of supra-Salado rock units, and assumes*
 33 *that vertical leakage (albeit very slow) occurs between rock units of the Rustler (where*
 34 *hydraulic gradients exist). Flow in the Culebra is considered transient, but is not expected to*
 35 *change significantly over the next 10,000 years. This differs from previous interpretations,*
 36 *wherein no flow was assumed between the Rustler units.*

37 *In an attachment to the May 14, 1997 letter, the DOE concluded that the presence of anhydrite*
 38 *within the Rustler units did not preclude slow downward infiltration, as previously argued by*
 39 *the DOE, and that the observed geochemistry and flow directions can be explained with*
 40 *different recharge areas and Culebra travel paths. The EPA reviewed the groundwater flow*
 41 *and recharge conceptualization and concluded that it provides a realistic representation of site*
 42 *conditions.*

43



• Observation Well
 Heads in meters
 Contour Interval:4m

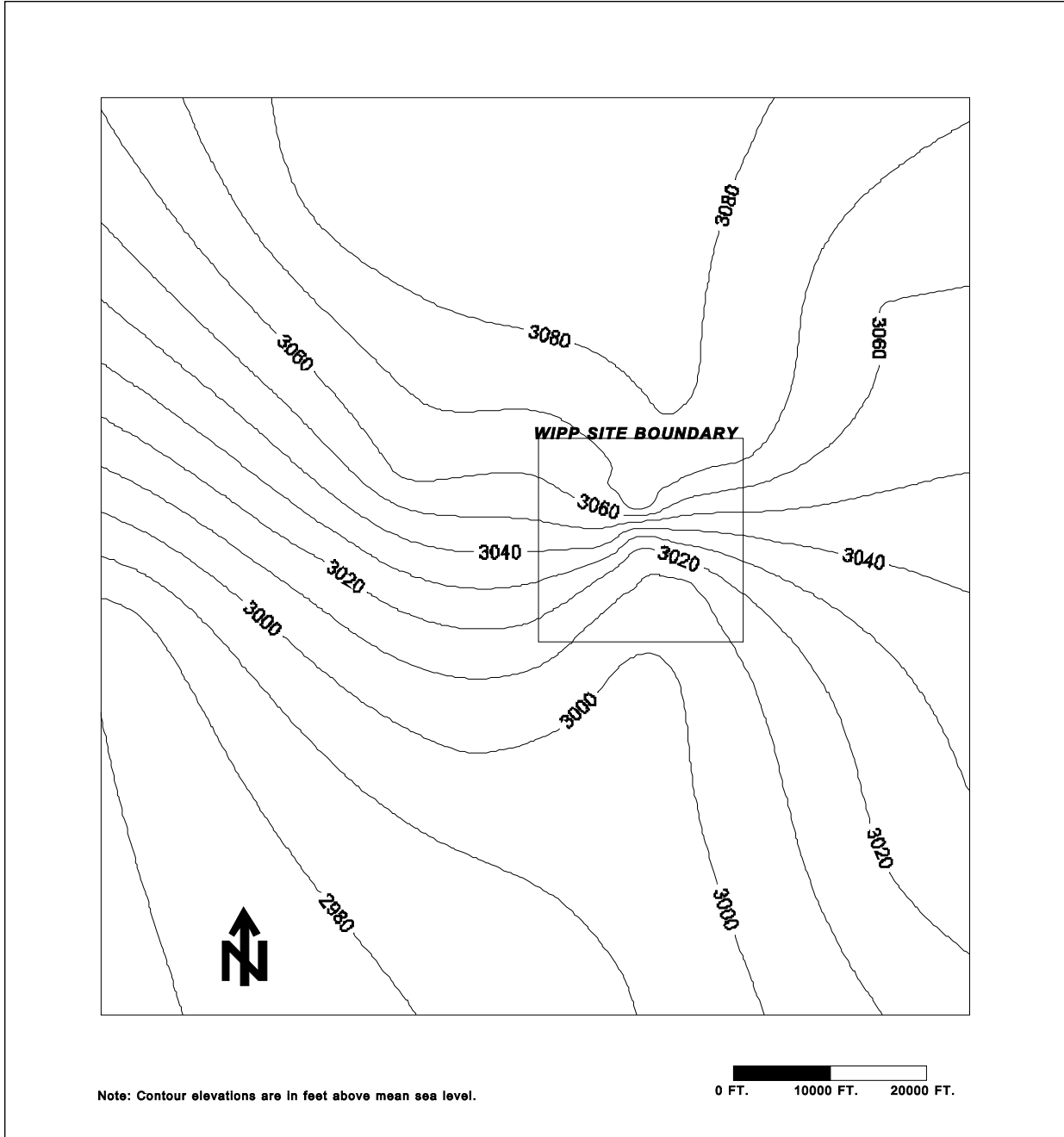


Note: Elevations in meters above the mean sea level
 adjusted to equivalent freshwater values.

CCA-047-2

1
 2
 3

Figure 2-31. Hydraulic Heads in the Culobra



1
2

Figure 2-37. Hydraulic Heads in the Culebra

3 *During the CCA review, the EPA found that information on the Culebra in the CCA lacked a*
4 *detailed discussion on the origin of the transmissivity variations relative to fracture*
5 *infil/dissolution, integration of climatic change, and loading/unloading events. These are*
6 *important aspects to understanding not only current transmissivity differences, but also*
7 *potential future transmissivity variations that could affect PA calculations. The EPA's review*
8 *stated, however, that the determination of the specific origin of fractures was not necessary*
9 *because conditions were not expected to change during the regulatory period.*

1 *The DOE provided supplemental information in letters in 1997 (Docket A-93-02, Items II-I-*
2 *03, II-I-24, II-I-31, II-H-44, and II-H-46) indicating that dissolution of fracture fill (which*
3 *has the potential to alter fracture permeability) is unlikely to occur. The EPA accepted the*
4 *DOE's position that infiltrating waters would most likely become saturated with calcium*
5 *sulfate and consequently would not dissolve anhydrite or gypsum fracture fill. Further*
6 *information on the EPA review of anhydrite and gypsum fracture fill dissolution is contained*
7 *in EPA Technical Support Document for Section 194.14: Content of Compliance*
8 *Certification Application, Section IV.C (Docket A-93-02, Item V-B-3).*

9 *The Sandia National Laboratories Annual Compliance Monitoring Parameter Assessment*
10 *reports the annual assessment of the Compliance Monitoring Parameters (COMPs) pursuant*
11 *to the SNL Analysis Plan, AP-069. The first assessment, for calendar year 1998 (SNL 2000a),*
12 *showed that changes in Culebra water levels were considered minor. During the assessment of*
13 *the COMP 'changes in groundwater flow' for calendar year 2001 (SNL 2002), estimated*
14 *freshwater Culebra heads in 15 wells were identified as above the ranges of uncertainty*
15 *estimated for steady-state conditions at those wells. At 8 of the 15 wells, the measured water*
16 *levels exceed the uncertainty range before being converted to freshwater head. In these cases,*
17 *conversion to freshwater head using any feasible fluid density can only increase the deviation*
18 *from the range. The freshwater head values from late 2000 were used to calibrate the Culebra*
19 *transmissivity (T) fields used to simulate the transport of radionuclides through the Culebra*
20 *(Appendix PA, Attachment TFIELD).*

21 *Because transport through the Culebra is a minor component of the total predicted releases*
22 *from the repository, these changes in head values have little or no effect on the total releases*
23 *to the accessible environment. The COMP assessment for the calendar year 2001 concluded*
24 *that the current head values do not indicate a condition adverse to the predicted performance*
25 *of the repository. However, because Culebra water levels are above expected values at most*
26 *wells, work has been initiated to investigate the reason for the change and further evaluate the*
27 *impact on performance.*

28 *Additional background for the Culebra model is in Appendix PA, Attachment TFIELD.*
29 *Additional information on long-term pumping test data is documented in Meigs et al. (2000)*
30 *and slug tests and short-term pumping tests are documented in Beauheim et al. (1991b) and*
31 *Beauheim and Ruskauff (1998).*

32 *Several new publications on the Culebra updating the original CCA information have been*
33 *released. Transport properties and tracer tests of the Culebra performed at the H-11 and H-19*
34 *hydropads are described in Meigs et al. (2000). The 1995-96 tracer test program, which*
35 *consisted of single-well injection-withdrawal tests and multiwell convergent flow tests, is*
36 *documented in Meigs and Beauheim (2001). The higher permeability of the lower Culebra*
37 *has been addressed in Meigs and Beauheim (2001, p. 1116).*

38 2.2.1.4.1.3 ~~The~~ Tamarisk

39 The Tamarisk acts as a confining layer in the groundwater basin model. Attempts were made in
40 two wells, H-14 and H-16, to test a 2.4-m (7.9-ft) sequence of the Tamarisk that consists of
41 claystone, mudstone, and siltstone overlain and underlain by anhydrite. Permeability was too

low to measure in either well within the time allowed for testing; consequently, Beauheim (1987a, *pp.* 108-110) estimated the transmissivity of the claystone sequence to be one or more orders of magnitude less than that of the tested interval in the ~~unnamed lower member~~ **Los Medaños** (that is, less than approximately $2.7 \times 10^{-11} \text{ m}^2/\text{sec}$ [$2.5 \times 10^{-5} \text{ ft}^2/\text{day}$]). The porosity of the Tamarisk was measured in 1995 as part of testing at the H-19 hydropad (TerraTek 1996). Two claystone samples had an effective porosity of 21.3 to 21.7 percent. Five anhydrite samples had effective porosities of 0.2 to 1.0 percent.

Fluid pressures in the Tamarisk have been measured continuously at well H-16 since 1987. From 1998 through 2002, the pressures increased approximately 20 psi, from 80 to 100 psi (185 to 230 ft of water), probably in a continuing recovery response to shaft grouting conducted in 1993 to reduce leakage. Given the location of the pressure transducer, the elevation of Tamarisk water level has increased from 899 to 913 m amsl (2,950 to 2,995 ft amsl) during this period. Currently, no other wells in the WIPP monitoring network are completed to the Tamarisk. Thus, H-16 provides the only information on Tamarisk head levels.

Similar to the Los Medaños, the Tamarisk includes a mudstone layer (M3/H3) that contains halite in some locations at and around the WIPP site. This layer is considered to be important because of the effect it has on the spatial distribution of transmissivity of the Culebra as described in Section 2.2.1.4.1.2. The M3/H3 margin is described in Section 2.1.3.5 and mapped in Figure 2-15.

The Tamarisk is incorporated into the conceptual model as discussed in Section 6.4.6.3. The role of the Tamarisk in the groundwater basin model is in **CCA** Appendix MASS, Section MASS.14.1. Tamarisk hydrological model parameters are in Appendix **PA, Attachment PAR**, Table PAR-2925.

2.2.1.4.1.4 ~~The~~ Magenta

The Magenta is a conductive hydrostratigraphic unit about 7.9 m (26 ft) thick at the WIPP. The Magenta is saturated except near outcrops along Nash Draw, and hydraulic data are available from ~~15~~ **22** wells *including 7 wells recompleted to the Magenta between 1995 and 2002 (SNL 2003a)*. According to Mercer (~~65~~ **CCA** Appendix HYDRO, *p.* 65), transmissivity ranges over five orders of magnitude from 1×10^{-9} to $4 \times 10^{-4} \text{ m}^2/\text{sec}$ (4×10^{-3} to $3.75 \times 10^2 \text{ ft}^2/\text{day}$). *A slug test performed in H-9c, a recompleted Magenta well (see Figure 2-5 for well location), yielded a transmissivity of $6 \times 10^{-7} \text{ m}^2/\text{s}$ ($0.56 \text{ ft}^2/\text{day}$), which is consistent with Mercer's findings (SNL 2003a)*. The porosity of the Magenta was measured in 1995 as part of testing at the H-19 hydropad (**TerraTek 1996**). Four samples had effective porosities ranging from 2.7 to 25.2 percent.

The hydraulic transmissivities of the Magenta, based on sparse data, show a decrease in ~~conductivity~~ from west to east, with slight indentations of the contours north and south of the WIPP that correspond to the topographic expression of Nash Draw. In most locations, the hydraulic conductivity of the Magenta is one to two orders of magnitude less than that of the Culebra. The Magenta does not have hydraulically significant fractures in the vicinity of the

1 WIPP. Treatment of the Magenta in the model is discussed in Section 6.4.6.4 with modeling
2 parameters in Table 6-224.

3 *Based on Magenta water levels measured in the 1980s (Lappin et al. 1989) when a wide*
4 *network of Magenta monitoring wells existed, the hydraulic gradient in the Magenta* across
5 the site varies from 3 to 4 m/km (16 to 20 ft/mi) on the eastern side, steepening to about 6 m/km
6 (32 ft/mi) along the western side near Nash Draw (Figure 2-3238).

7 Regional modeling using the groundwater basin model indicates that leakage occurs into the
8 Magenta from the overlying Forty-niner and out of the Magenta downwards into the Tamarisk.
9 Regional modeling also indicates that flow directions in the Magenta are dominantly westward,
10 similar to the slope of the land surface in the immediate area of the WIPP. This flow direction is
11 different than the dominant flow direction in the next underlying conductive unit, the Culebra.
12 This difference is consistent with the groundwater basin conceptual model, in that flow in
13 shallower units is expected to be more sensitive to local topography.

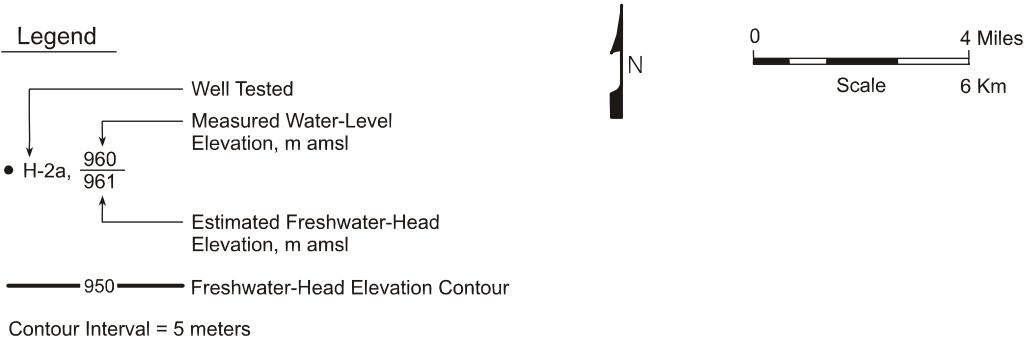
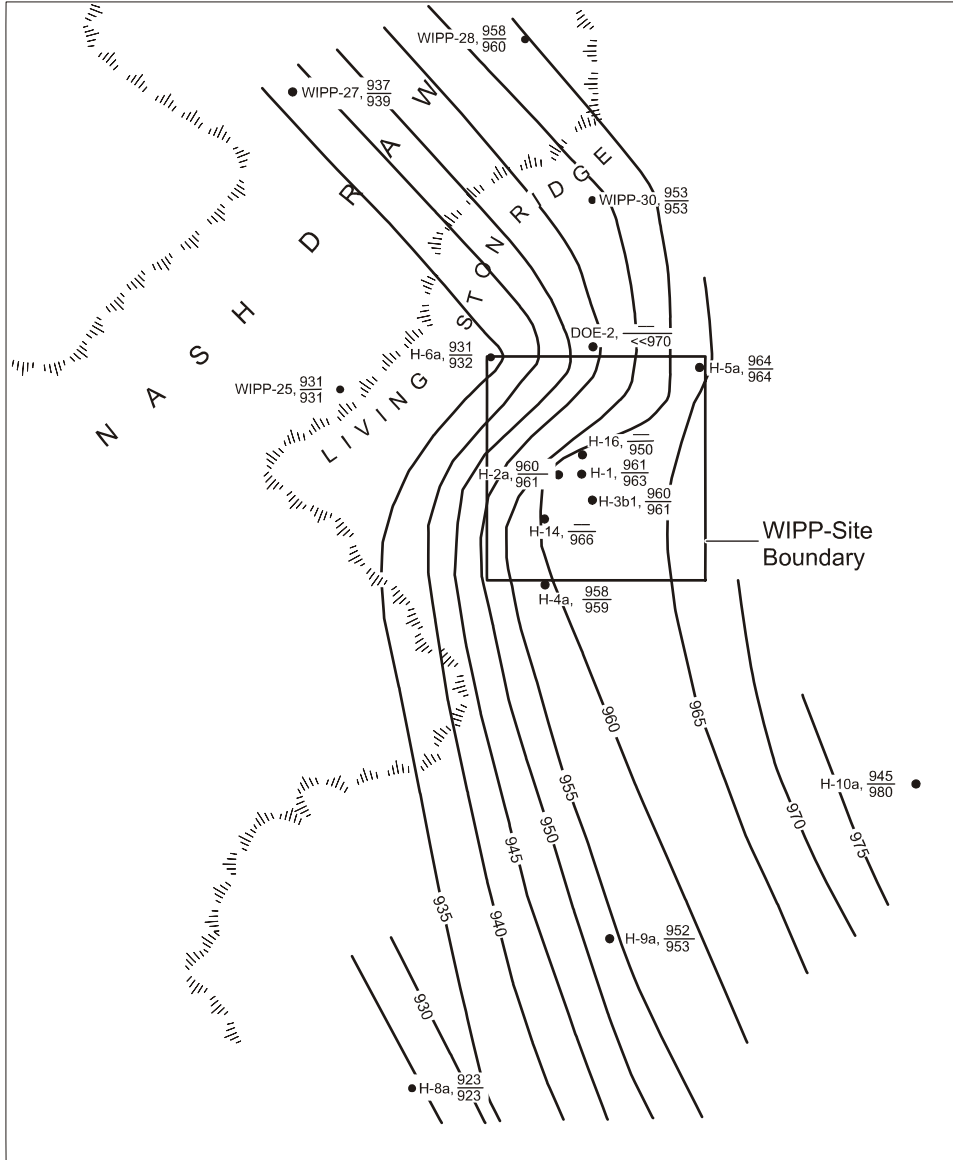
14 Inferences about vertical flow directions in the Magenta have been made from well data
15 collected by the DOE. Beauheim (1987a, p. 137) reported flow directions downwards out of the
16 Magenta over the WIPP site, consistent with results of groundwater basin modeling.

17 However, Beauheim (1987a, p. 139) concluded that flow directions between the Forty-niner and
18 Magenta would be upward in the three boreholes from which reliable pressure data are available
19 for the Forty-niner (H-3, H-14, and H-16), which is not consistent with the results of
20 groundwater modeling. This inconsistency may be the result of local heterogeneity in rock
21 properties that affect flow on a scale that cannot be duplicated in regional modeling.

22 As is the case for the Culebra, groundwater elevations in the Magenta have changed over the
23 period of observation. The pattern of changes is similar to that observed for the Culebra (*see*
24 *Section 2.2.1.4.1.2*), and is *being investigated under the current DOE hydrology program (SNL*
25 *2003b)*. ~~attributed to the same causes (see Section 2.2.1.4.1.2).~~

26 2.2.1.4.1.5 ~~The~~ Forty-niner

27 The Forty-niner is a confining hydrostratigraphic layer about 20 m (66 ft) thick throughout the
28 WIPP area and consists of low-permeability anhydrite and siltstone. Tests by Beauheim (1987a,
29 119-123 and Table 5-2) in H-14 and H-16 yielded transmissivities of about 3×10^{-8} to 8×10^{-8}
30 m^2/sec (3×10^{-2} to 7×10^{-2} ft^2/day) and 3×10^{-9} to 6×10^{-9} m^2/sec (5×10^{-3} to 6×10^{-3} ft^2/day),
31 respectively, *for the medial siltstone unit of the Forty-niner. Tests of the siltstone in H-3d*
32 *provided transmissivity estimates of 3.8×10^{-9} to 4.8×10^{-9} m^2/s (3.5×10^{-3} to 4.5×10^{-3} ft^2/day)*
33 *(Beauheim et al. 1991b, Table 5-1). The porosity of the Forty-niner was measured as part of*
34 *testing at the H-19 hydropad (TerraTek 1996). Three claystone* samples had effective
35 porosities ranging from 9.1 to 24.0 percent. Four anhydrite samples had effective porosities
36 ranging from 0.0 to 0.4 percent. Model consideration of the Forty-niner is in Section 6.4.6.5.
37 Modeling parameters are in *CCA* Appendix PAR, Table PAR-27.



1

2

Figure 2-3238. Hydraulic Heads in the Magenta (1980s)

CCA-048-2